![THE UNIVERSITY of EDINBURGH]

Edinburgh Research Explorer

Neuroinvasion by scrapie following inoculation via the skin is independent of migratory Langerhans cells

Link:
Link to publication record in Edinburgh Research Explorer

Document Version:
Publisher's PDF, also known as Version of record

Published In:
J Virol

OPEN ACCESS

Vol. 79, No. 3

Neuroinvasion by Scrapie following Inoculation via the Skin Is Independent of Migratory Langerhans Cells

Joanne Mohan, Moira E. Bruce, and Neil A. Mabbott*

Neuropathogenesis Unit, Institute for Animal Health, Edinburgh, Scotland, United Kingdom

Many natural transmissible spongiform encephalopathy (TSE) infections are likely to be acquired peripherally, and studies in mice show that skin scarification is an effective means of scrapie transmission. After peripheral exposure, TSE agents usually accumulate in lymphoid tissues before spreading to the brain. The mechanisms of TSE transport to lymphoid tissues are not known. Langerhans cells (LCs) reside in the epidermis and migrate to the draining lymph node after encountering antigen. To investigate the potential role of LCs in scrapie transportation from the skin, we utilized mouse models in which their migration was blocked either due to CD40 ligand deficiency (CD40L$^{-/-}$ mice) or after caspase-1 inhibition. We show that the early accumulation of scrapie infectivity in the draining lymph node and subsequent neuroinvasion was not impaired in mice with blocked LC migration. Thus, LCs are not involved in TSE transport from the skin. After intracerebral inoculation with scrapie, wild-type mice and CD40L$^{-/-}$ mice develop clinical disease with similar incubation periods. However, after inoculation via skin scarification CD40L$^{-/-}$ mice develop disease significantly earlier than do wild-type mice. The shorter incubation period in CD40L$^{-/-}$ mice is unexpected and suggests that a CD40L-dependent mechanism is involved in impeding scrapie pathogenesis. In vitro studies demonstrated that LCs have the potential to acquire and degrade protease-resistant prion protein, which is thought to be a component of the infectious agent. Taken together, these data suggest that LCs are not involved in scrapie transport to draining lymphoid tissues but might have the potential to degrade scrapie in the skin.

The transmissible spongiform encephalopathies (TSEs; or prion diseases) are a group of infectious, fatal, neurodegenerative diseases, which affect both animals and humans. During disease, PrP^{Sc}, an abnormal, detergent-insoluble, relatively proteinase-resistant isoform of the host glycoprotein PrP^C (38) accumulates in infected tissues. The deposition of PrP^{Sc} within the brains of most TSE-affected hosts is usually accompanied with the development of neuropathological changes, such as vacuolation, gliosis, and neuronal loss. Although the precise nature of the TSE agent is not known, PrP^{Sc} accumulates with infectivity in infected tissues and is considered to be a major or possibly the sole component of the infectious agent (44).

Many TSEs, including natural sheep scrapie, bovine spongiform encephalopathy (BSE), chronic wasting disease in mule deer and elk, and variant Creutzfeldt-Jakob disease (vCJD) in humans, are acquired by peripheral exposure. For example, the consumption of BSE-contaminated meat products by humans is most likely responsible for the emergence of vCJD (7, 22). Although many natural TSE infections are likely to be acquired orally, studies in mice show that skin scarification is also an effective means of scrapie transmission (51). This suggests some natural TSE cases might be transmitted through skin lesions in the mouth (3) or through sites of skin trauma during close contact with infected animals. The potential to transmit vCJD in humans iatrogenically during surgical or dental procedures is a current concern.

Early PrP^{Sc} accumulation takes place on follicular dendritic cells (FDCs) within germinal centers in lymphoid tissues of

patients with vCJD (21), in mule deer with chronic wasting disease (47), in sheep with natural scrapie (55), and in rodents inoculated with scrapie by peripheral routes (6, 33, 37). In mouse scrapie models, mature FDCs are critical for scrapie replication and PrP^{Sc} accumulation in lymphoid tissues and, in their absence, neuroinvasion after peripheral challenge is significantly impaired (6, 32, 39, 51). From the lymphoid tissues, scrapie is translocated to the central nervous system (CNS) via peripheral nerves (20, 42).

Scrapie neuroinvasion after inoculation into the skin does not occur through direct uptake by nerves in the skin since highly immunodeficient SCID mice are refractory to scrapie when inoculated by this route (51). These data confirm that after inoculation via the skin, neuroinvasion occurs after accumulation in lymphoid tissues as demonstrated after inoculation by other peripheral routes (6, 34). How TSE agents are initially transported from the site of exposure, such as the gastrointestinal tract or the skin, to the germinal centers in which they replicate is not known. FDCs could directly trap cell-free PrP^{Sc} or other agent-associated molecules in a complement-bound complex (28, 31), but it is also possible that mobile cells transport the agent to lymphoid follicles. Several cells have the potential to transport TSE agents, including macrophages and migratory bone marrow-derived dendritic cells (DCs). The evidence that macrophages destroy infectivity and degrade PrP^{Sc} makes them an unlikely and inefficient transport candidate (4, 10, 11). Migratory bone marrow-derived DCs are a distinct lineage from tissue-fixed, stroma-derived FDCs, which are not considered to be of hemopoietic origin (14, 25). These DCs continually circulate throughout the host's tissues and tissue fluids, where they sample antigens and transport them to lymphoid tissues (2). Unlike macrophages, DCs can retain some

* Corresponding author. Mailing address: Institute for Animal Health, Neuropathogenesis Unit, Ogston Bldg., West Mains Rd., Edinburgh EH9 3JF, United Kingdom. Phone: 44(0)131-667-5204. Fax: 44(0)131-668-3872. E-mail: neil.mabbott@bbsrc.ac.uk.

protein antigens in native, nondegraded form (57). A subpopulation of these migratory DCs has been shown to transport intestinally injected PrP^{Sc} to mesenteric lymph nodes via the lymph (23), but direct demonstration of their involvement in TSE pathogenesis is lacking.

Langerhans cells (LCs) are a subset of migratory DCs that reside in the epidermis and migrate to the draining lymph node following antigen encounter (2). DCs, including LCs, are considered to provide potential mechanisms for the transmission of some pathogens into the skin such as dengue virus (56), human immunodeficiency virus (45), maedi-visna lentivirus (46), and Venezuelan equine encephalitis virus (35). These characteristics suggested to us that LCs are plausible candidates for scrapie transport from the skin to draining lymph nodes. LCs require a number of stimuli to induce their mobilization out of the skin (2). The CD40-CD40L signaling pathway is just one component in a complex network of stimuli that regulate the migration of antigen-bearing LCs out of the epidermis to the draining lymph node (40). In mice deficient in CD40 ligand (CD40L$^{-/-}$ mice), the number and morphology of LCs in the epidermis is normal, but they fail to migrate from the skin and do not accumulate in the draining lymph node (40). Likewise, caspase-1 plays an important role in the regulation of LC migration, and its specific inhibition blocks LC migration from the epidermis (1). In order to investigate the potential role of LCs in scrapie transportation from skin to draining lymphoid tissues, we studied pathogenesis in models in which the migration of these cells from the epidermis was impaired, either due to CD40L deficiency (40) or to caspase-1 inhibition (1). We used these models to investigate the potential role of LCs in scrapie pathogenesis after inoculation via the skin with doses of scrapie equivalent to and much lower than those previously shown to require amplification in lymphoid tissues prior to neuroinvasion (31, 32, 51).

MATERIALS AND METHODS

Mice. CD40 ligand-deficient (CD40L$^{-/-}$) mice (58) were bred and maintained on the C57BL/6 background. Age- and sex-matched C57BL/6 mice were used as wild-type control mice in studies with CD40L$^{-/-}$ mice. Another subline of C57BL mice, C57BL/Dk mice, were used in all other studies. All mice were housed under specific-pathogen-free conditions.

Scrapie inoculation. Mice (8 to 12 weeks of age) were inoculated with the ME7 scrapie strain by skin scarification of the medial surface of the right thigh. Briefly, prior to scarification ~1 cm^2 of hair covering the scarification site was trimmed by using curved scissors and then removed completely with an electric razor. After 24 h a 23-gauge needle was used to create a 5-mm abrasion in the epidermal layers of the skin at the scarification site. Care was taken to avoid damage to the dermis or drawing blood during scarification. Then, by using a 26-gauge needle, one droplet (~6 μl) of ME7 scrapie mouse brain homogenate containing ca. 10^4 or 10^3 50% infectious dose (ID$_{50}$) units was applied to the abrasion and worked into the site by using sweeping strokes. The scarification site was then sealed with OpSite (Smith & Nephew Medical, Ltd., Hull, United Kingdom) and allowed to dry before the animals were returned to their final holding cages. Where indicated, separate groups of mice were inoculated by intracerebral (i.c.) injection with 20 μl of scrapie mouse brain homogenate containing ca. 10$^{4.5}$ ID$_{50}$ units as a titer control. After challenge, animals were coded, assessed weekly for signs of clinical disease, and killed at a standard clinical endpoint (17). Scrapie diagnosis was confirmed by histopathologic assessment of TSE vacuolation in the brain. For the construction of lesion profiles, vacuolar changes were scored in nine gray-matter and three white-matter areas of the brain as described previously (18).

Where indicated, some mice were sacrificed 49 days postinoculation, and spleens and inguinal lymph nodes (ILNs) taken for further analysis. For bioassay of scrapie infectivity, two half spleens were pooled from each group and prepared

as 10% (wt/vol) homogenates in physiological saline. Likewise, the ILNs draining the inoculation site were pooled from two mice and prepared as a 10% (wt/vol) homogenate. Groups of 12 C57BL/Dk indicator mice were injected i.c. with 20 μl of each homogenate. The scrapie titer in each sample was determined from the mean incubation period in the assay mice by reference to established dose-incubation period response curves for scrapie-infected spleen tissue.

Caspase inhibitor treatment. Where indicated, prior to inoculation with scrapie by skin scarification, groups of C57BL/Dk mice were pretreated at the shaved inoculation site with 50 μl of 0.4 mM caspase-1 inhibitor II (Ac-YVAD-cmk; Calbiochem, Beeston, United Kingdom), 0.4 mM caspase-3 inhibitor III (Ac-DEVD-cmk; Calbiochem), or vehicle alone (dimethyl sulfoxide [DMSO]) by using a previously established protocol (1). One hour later, mice were inoculated with scrapie as described above. Care was taken to ensure that the scrapie inoculum was only applied to the pretreated area of skin.

Immunohistochemical analysis. To monitor FDC status, spleen halves were snap-frozen at the temperature of liquid nitrogen. Serial frozen sections (thickness, 10 μm) were cut on a cryostat, and FDCs were visualized by staining with either the FDC-specific rat monoclonal antiserum FDC-M2 (AMS Biotechnology, Oxon, United Kingdom) or 8C12 monoclonal antiserum to detect CD35 (BD Biosciences Pharmingen, Oxford, United Kingdom). B lymphocytes were detected by using the rat B220 monoclonal antiserum to detect CD45R (Caltag, Towcester, United Kingdom) or biotin-conjugated peanut agglutinin (PNA; Sigma, Poole, United Kingdom) to detect germinal center B lymphocytes. Immunolabeling was carried out with alkaline phosphatase coupled to the avidin-biotin complex (Vector Laboratories, Burlingame, Calif.). Vector Red (Vector Laboratories) was used as a substrate.

For the detection of PrP in the brain, tissues were fixed in periodate-lysine-paraformaldehyde and embedded in paraffin wax. Sections (thickness, 6 μm) were deparaffinized and then pretreated to enhance PrP immunostaining by hydrated autoclaving (15 min, 121°C, hydration) and subsequent immersion in formic acid (98%) for 5 min (37). Sections were then stained with the PrP-specific monoclonal antiserum 6H4 (Prionics, Zurich, Switzerland), and immunolabeling was detected by using hydrogen peroxidase coupled to the avidin-biotin complex (Vector Laboratories) with diaminobenzidine as a substrate. Glial fibrillary acid protein (GFAP) was detected on adjacent brain sections by using rabbit GFAP-specific antiserum (Dako, Ltd., Ely, United Kingdom), and immunolabeling carried out by using alkaline phosphatase coupled to the avidin-biotin complex by using Vector Red as a substrate. Microglia were detected by staining with biotin-conjugated *Lycopersicon esculentum* agglutinin (LEA; Sigma), and specific labeling was detected by using hydrogen peroxidase coupled to the avidin-biotin complex with diaminobenzidine as a substrate.

All sections were counterstained with hematoxylin to distinguish cell nuclei.

Immunoblot detection of PrP^{Sc}. Individual spleen fragments or ILNs were prepared as previously described (15). Briefly, before immunoblot analysis, tissue homogenates were treated in the absence or presence of 80 μg of proteinase K (to confirm the presence of PrP^{Sc}), electrophoresed through sodium dodecyl sulfate–10 to 20% polyacrylamide gels (Bio-Rad, Hemel Hempstead, United Kingdom), and transferred to polyvinylidene difluoride membranes (Bio-Rad) by semidry blotting. PrP was detected with the PrP-specific mouse monoclonal antiserum 8H4 (61). Immunolabeling was carried out with horseradish peroxidase-conjugated goat anti-mouse immunoglobulin G antiserum (Jackson Immunoresearch Laboratories, Inc., West Grove, Pa.), and bound horseradish peroxidase activity was detected with Supersignal West Dura Extended Duration Substrate (Pierce, Chester, United Kingdom).

Cell culture. The XS106 and XS52 cell lines (54, 59) are long-term DC lines established from the epidermis of newborn A/J mice and BALB/c mice, respectively. XS106 cells were expanded and maintained in complete RPMI 1640 (60) supplemented with 0.5 ng of recombinant murine granulocyte monocyte colony-stimulating factor (R&D Systems, Abingdon, United Kingdom)/ml and 5% (vol/vol) NS47 fibroblast culture supernatant. XS52 cells were expanded and maintained in complete RPMI 1640 supplemented with 2.0 ng of recombinant murine granulocyte monocyte colony-stimulating factor/ml and 10% (vol/vol) NS47 fibroblast culture supernatant/ml. Both cell lines were cultivated at 37°C in a 5% CO$_2$–air atmosphere. For scrapie inoculation studies, sterile coverslips were placed in the wells of a 24-well plate (Corning, Buckinghamshire, United Kingdom). Cells (5 × 10^5 in 1 ml of medium) were seeded into each well. When confluent (ca. 2 × 10^6 cells per coverslip), each well was then inoculated with 10 μl of 10% (wt/vol) terminal scrapie mouse brain homogenate in complete RPMI (equivalent to 1.0 mg of tissue). Duplicate sets of cultures cells were inoculated with 10 μl of 10% (wt/vol) uninfected mouse brain homogenate in complete RPMI as a control. The medium was removed after 16 h of incubation at 37°C in a 5% CO$_2$–air atmosphere, and cells in each well were washed extensively with fresh medium by pipetting. The cells were then incubated at 37°C for the times

indicated before being assayed for PrP^{Sc} accumulation by the cell blot procedure (5). Briefly, coverslips were removed, and the cell-containing side was blotted onto polyvinylidene difluoride membranes, treated with proteinase K, denatured with guanidine isothiocyanate, and PrP detected by using the PrP-specific mouse monoclonal antiserum 8H4 (61). Immunolabeling was carried out with horseradish peroxidase-conjugated goat anti-mouse IgG antiserum (Jackson Immunoresearch Laboratories), and bound horseradish peroxidase activity was detected with Supersignal West Dura Extended Duration Substrate (Pierce). After exposure, membranes were stained with 0.5 μg of ethidium bromide/ml and observed in UV light to confirm transfer of the cell layer (13). Cell viability was assessed in duplicate sets of cultures by trypan blue dye exclusion, and metabolic activity was measured by using Alamarblue (Serotec, Oxford, United Kingdom).

Statistical analysis. Where indicated, the incubation periods are presented as mean (days) ± the standard error of the mean. Significant differences between incubation periods in different groups were determined by one-way analysis of variance (ANOVA) with Minitab for Windows software (Minitab, Inc., State College, Pa.).

RESULTS

Effect of caspase-1 inhibition on scrapie pathogenesis. Previous studies have shown that topical treatment with a pharmacological inhibitor of caspase-1 potently blocks LC migration from the skin (1). Therefore, we investigated whether the accumulation of scrapie in the draining lymph node was affected after topical caspase-1 inhibition. Prior to inoculation with scrapie by skin scarification (6 μl containing ca. 10^4 ID$_{50}$ units), C57BL/Dk mice were treated at the inoculation site with Ac-YVAD-cmk, a cell-permeable, irreversible caspase-1 inhibitor (19, 53), according to a previously established protocol (1). This treatment effectively and irreversibly blocks both spontaneous and induced LC migration from the epidermis (1). Control pretreatments included application of Ac-DEVD-cmk, a specific inhibitor of caspase-3 that has little effect on caspase-1 (19), vehicle alone (DMSO), or no pretreatment. After peripheral inoculation of immunocompetent mice with the ME7 scrapie strain, high levels of infectivity accumulate in lymphoid tissues within the first few weeks postinoculation and are maintained throughout the course of infection (6, 33). Our studies suggest that after inoculation via skin scarification, the infectivity levels in the draining ILNs begin to peak around 49 days postinoculation and subsequently plateau (unpublished data). Therefore, in the present study, ILNs draining the site of inoculation were taken from two mice from each treatment group 49 days after inoculation and scrapie infectivity titers in pooled ($n = 2$) tissue homogenates were estimated by bioassay in indicator mice. As expected, ILNs from untreated mice contained high levels of scrapie infectivity (ca. 6.7 log i.c. ID$_{50}$/ g). If we assume that analyses of scrapie infectivity in indicator mice have a standard deviation of ±0.5 log i.c. ID$_{50}$/g, this margin of error was used as a threshold above or below which differences between samples were considered significant. However, our studies clearly demonstrated that infectivity titers in ILNs from Ac-YVAD-cmk-pretreated mice (ca. 6.4 log i.c. ID$_{50}$/g) were similar to those from untreated mice, indicating that pharmacological blockade of caspase-1-dependent LC migration from the skin did not affect the early accumulation of scrapie infectivity in ILNs. Likewise, no effect on the early accumulation of scrapie infectivity in ILNs was observed in mice pretreated with Ac-DEVD-cmk or DMSO alone as controls compared to Ac-YVAD-cmk-pretreated mice or untreated control mice. Tissues from mice treated with DEVD-cmk or DMSO alone each contained infectivity titers of ca. 6.0

TABLE 1. Treatment of skin with the caspase-1 inhibitor Ac-YVAD-cmk to block LC migration prior to scrapie inoculation by skin scarification does not affect disease susceptibility[a]

Pretreatment[b]	Incidence[c]	Mean incubation period (days) ± SE	Statistical analysis[d]
None	9/9	316 ± 2	
DMSO	10/10	323 ± 4	0.186
Ac-YVAD-cmk	14/14	323 ± 4	0.192
Ac-DEVD-cmk	10/10	316 ± 3	0.774

[a] C57BL/Dk mice were inoculated with the ME7 scrapie strain (10^4 ID$_{50}$ units) by skin scarification of the medial surface of the right thigh.

[b] Prior to scrapie inoculation mice were pretreated at the shaved inoculation site with Ac-YVAD-cmk (a caspase-1 inhibitor) or Ac-DEVD-cmk (a caspase-3 inhibitor) or vehicle alone (DMSO) as controls.

[c] That is, the number of animals affected/the total number of animals inoculated.

[d] Degrees of significance between the mean incubation periods for each treatment group compared to untreated control mice (None) were determined by ANOVA. Values represent P values, where $P \leq 0.05$ was considered significant different.

log i.c. ID$_{50}$/g. Consistent with the finding that caspase-1 inhibition did not affect the early accumulation of scrapie in lymph nodes after inoculation via skin scarification, Ac-YVAD-cmk pretreatment did not significantly affect the incubation period or disease susceptibility compared to untreated control mice ($P \leq 0.192$, $n = 9$ [ANOVA]). Likewise, treatment of mice with the control reagents Ac-DEVD-cmk or DMSO alone also did not significantly affect the incubation period or disease susceptibility compared to untreated control mice ($P \leq 0.774$ [$n = 10$] and $P \leq 0.148$ [$n = 10$], respectively [ANOVA]). Mice from each treatment group developed clinical scrapie with similar incubation periods between 316 and 323 days (Table 1).

Lymphoid tissues of CD40L$^{-/-}$ mice contain FDCs but lack germinal centers. We next investigated scrapie pathogenesis in mice with a permanent block in LC migration out of the skin due to a targeted deletion of the CD40L gene (CD40L$^{-/-}$ mice [40]). CD40L$^{-/-}$ mice are incapable of mounting T-cell-dependent humoral immune responses, and germinal center development is impaired (58). Therefore, FDC status was first assessed in spleens from C57BL/6 wild-type mice and CD40L$^{-/-}$ mice. Germinal centers containing PNA-binding B lymphocytes were detected in the spleens of all C57BL/6 wild-type mice but not in the spleens of CD40L$^{-/-}$ mice (Fig. 1a). Despite the impaired germinal center formation in the lymphoid tissues of CD40L$^{-/-}$ mice, mature FDC networks surrounded by B lymphocytes (CD45R/B220 positive cells) were detected (Fig. 1b). Expression of the markers FDC-M2 and CD35 by FDCs in spleens of CD40L$^{-/-}$ mice appeared to be similar to that observed in lymphoid tissues from C57BL/6 wild-type mice (Fig. 1b).

Effect of CD40L deficiency on scrapie accumulation in lymphoid tissues. We next studied the early delivery of scrapie from the skin to the draining lymphoid tissues in the absence of migratory LCs in CD40L$^{-/-}$ mice. In the present study, ILNs draining the site of inoculation and spleens were taken from two wild-type mice and from two CD40L$^{-/-}$ mice 49 days after inoculation with scrapie by skin scarification (6 μl containing ca. 10^4 ID$_{50}$ units). The scrapie infectivity titers in pooled ($n = 2$) tissue homogenates were estimated by bioassay in groups of 12 indicator mice. As expected, draining ILNs from wild-type
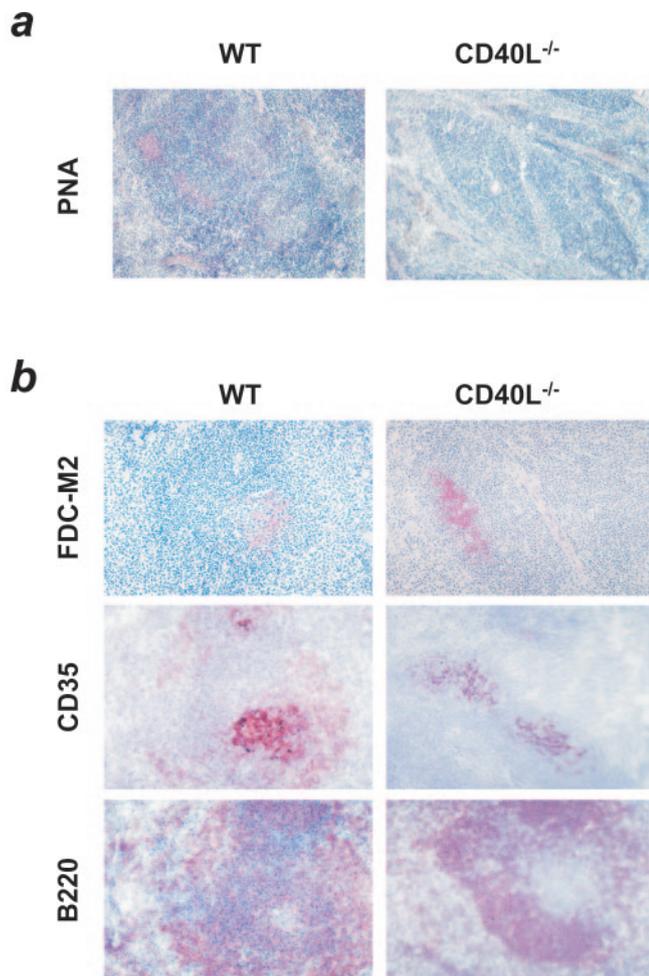
a

b

FIG. 1. Germinal center architecture in the spleens of C57BL/6 wild-type (WT) and CD40L$^{-/-}$ mice. (a) Immunohistochemical analysis detected the presence of PNA-positive germinal center B lymphocytes in the spleens of WT mice (red; left panel) but not in tissue from CD40L$^{-/-}$ mice (right panel). Magnification, ×100. (b) Immunohistochemical analysis of FDC networks in spleen tissue from wild-type (left panels) and CD40L$^{-/-}$ mice (right panels). Adjacent frozen sections were stained with FDC-M2 (upper row; red) monoclonal antiserum to detect FDCs, 8C12 monoclonal antiserum to detect CD35 (middle row; red), and B220 monoclonal antiserum to detect B lymphocytes (lower row; red). Magnification, ×200. All sections were counterstained with hematoxylin (blue).

mice contained high levels of scrapie infectivity (ca. 5.8 log i.c. ID$_{50}$/g). Again, to compare infectivity titers between groups, a standard deviation of ±0.5 log i.c. ID$_{50}$/g was used as a threshold above or below which samples were considered significantly different. Our data suggested that in the absence of efficient LC migration from the skin the early accumulation of scrapie infectivity in the draining ILN was not impaired, since high levels of infectivity were also detected in samples of ILNs from CD40L$^{-/-}$ mice taken 49 days postinoculation (ca. 5.9 log i.c. ID$_{50}$/g).

Only trace levels of infectivity (<2.0 log i.c. ID$_{50}$/g) were detected in pooled spleen samples from the same wild-type mice and CD40L$^{-/-}$ mice taken 49 days postinoculation. However, at the terminal stage of disease, abundant detergent-
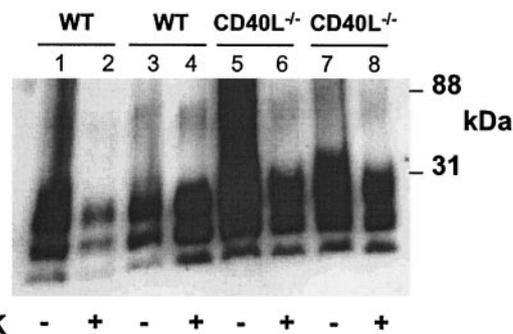

FIG. 2. PrP^{Sc} accumulation in spleen tissue from terminally scrapie-infected C57BL/6 wild-type (WT) and CD40L$^{-/-}$ mice inoculated with scrapie by skin scarification. Immunoblots show the accumulation of detergent-insoluble, relatively proteinase K-resistant PrP^{Sc}. The treatment of tissues in the presence (+) or absence (−) of proteinase K prior to electrophoresis is indicated. After proteinase K treatment, a typical three-band pattern was observed between the molecular mass values of 20 and 30 kDa, representing the unglycosylated, monoglycosylated, and diglycosylated isomers of PrP (in order of increasing molecular mass). PK, proteinase K.

insoluble, relatively proteinase K-resistant accumulations of disease-specific PrP^{Sc} were detected in spleens from wild-type mice (Fig. 2, lanes 2 and 4) and CD40L$^{-/-}$ mice (Fig. 2, lanes 6 and 8). Taken together, these data demonstrate that after inoculation via the skin, infectivity is propagated to the draining lymph node via the lymphatics in an LC-independent manner and subsequently distributed to the spleen, probably via the bloodstream. Since only trace levels of infectivity are measured in the spleen at a time when high levels of infectivity are detected in the draining lymph node, these data suggest that the initial transmission from the skin to local lymphoid tissues does not occur via the bloodstream.

Susceptibility of CD40L$^{-/-}$ mice to scrapie infection. When mice were challenged i.c. with a moderate dose of scrapie (10$^{4.5}$ ID$_{50}$ units), wild-type mice and CD40L$^{-/-}$ mice developed clinical signs of scrapie with similar incubation periods of 159 to 165 days (Table 2). Histopathologic analysis of brain tissue from terminally affected wild-type and CD40L$^{-/-}$ mice displayed the characteristic spongiform pathology, disease-specific PrP accumulation, and reactive astrocytes expressing the high levels of GFAP typical of an i.c. inoculation with the ME7 scrapie strain, although microglia activation appeared more pronounced in the brains of CD40L$^{-/-}$ mice (data not shown). However, the severity and distribution of pathological vacuolation in the brain was not significantly different between mouse strains (Fig. 3a). Thus, these data suggest that the CD40L signaling pathway is not involved in the cerebral pathogenesis of the ME7 scrapie strain.

After inoculation with scrapie by skin scarification, CD40L$^{-/-}$ mice developed clinical disease significantly earlier than immunocompetent wild-type mice (Table 2). For example, following inoculation with a moderate dose of scrapie (10^4 ID$_{50}$ units), all immunocompetent wild-type mice developed clinical signs of scrapie with a mean incubation period of 344 ± 5 days (n = 8). In contrast, CD40L$^{-/-}$ mice developed clinical scrapie 32 days earlier than the wild-type controls, with a mean incubation period of 312 ± 5 days (P ≤ 0.0003, n = 9 [ANOVA]). Characteristic spongiform pathology and disease-

TABLE 2. Susceptibility of wild-type (C57BL/6) and CD40L$^{-/-}$ mice to scrapie after inoculation via skin scarification or i.c. injection[a]

Mouse strain	Skin scarification[b]				i.c. inoculation ($10^{4.5}$ ID$_{50}$ units)	
	10^4 ID$_{50}$ units		10^3 ID$_{50}$ units			
	Scrapie incidence	Incubation period	Scrapie incidence	Incubation period	Scrapie incidence	Incubation period
C57BL/6	8/8	344 ± 5	8/9[c]	355 ± 13	5/5	165 ± 1
CD40L$^{-/-}$	9/10[d]	312 ± 5	7/8[e]	331 ± 6	6/6	159 ± 1

[a] Scrapie incidence is expressed as the number of animals with scrapie/total number of animals inoculated. The incubation period is expressed as the mean number of days ± the standard error of the mean.

[b] Mice were inoculated with the ME7 scrapie strain by skin scarification of the medial surface of the right thigh.

[c] One mouse remained free from the signs of scrapie for 504 days postinoculation, at which point the experiment was terminated. No histopathologic signs of scrapie were detected in the brain (data not shown).

[d] One mouse died at 306 days postinoculation. No histopathologic signs of scrapie were detected in the brain (data not shown).

[e] One mouse died at 359 days postinoculation. No histopathologic signs of scrapie were detected in the brain (data not shown).

specific PrP accumulations typical of an infection with the ME7 scrapie strain were detected in the brains of all peripherally inoculated wild-type and CD40L$^{-/-}$ mice (Fig. 4). Although the activation status of LEA-binding microglia appeared more pronounced in the brains of CD40L$^{-/-}$ mice compared to wild-type mice (Fig. 4), no significant difference in the severity or distribution of the vacuolation in the brain was observed between mouse strains (Fig. 3b). Thus, the shortened incubation period in CD40L$^{-/-}$ mice was unlikely to be attributed to an exaggerated neuropathology in these mice compared to wild-type mice. After peripheral inoculation with a limiting dose of scrapie (10^3 ID$_{50}$ units), CD40L$^{-/-}$ mice also developed clinical scrapie sooner than wild-type mice (Table 2). Although CD40L$^{-/-}$ mice succumbed to scrapie after inoculation with a limiting dose of scrapie with a mean incubation period of 331 ± 6 days ($n = 7$), 24 days earlier than wild-type mice (355 ± 13 days, $n = 8$), the difference between the two groups in this instance was not significant ($P \leq 0.075$ [ANOVA]). This is most likely a consequence of the wide scatter of incubation periods for the wild-type mice from 336 to 439 days.

Skin-derived LC-like cells degrade PrP^{Sc} in vitro. A series of long-term DC lines have been generated from murine skin that retain important features of LCs (54, 59). In the present study, we used the skin-derived LC-like cell lines XS106 and XS52. The XS106 cells express moderate levels of Ia molecules, CD40, CD80, and CD86 and are capable of stimulating immune responses after adoptive transfer (54). Monolayers of XS106 cells were inoculated with a suspension of terminally ME7-scrapie infected brain tissue or normal brain tissue (as a control). After 16 h of incubation, culture medium was aspirated, and cells were washed extensively with fresh medium to remove residual inoculum. Fresh medium was then added to the monolayers, and cells were incubated for up to 96 h. The experiment demonstrated that 24 h after inoculation with scrapie, XS106 LC-like cells had acquired and retained high levels of PrP^{Sc} (Fig. 5a). No PrP^{Sc} accumulations were detected in association with cells exposed to normal brain homogenate as a control (Fig. 5a). As a further control, cell-free
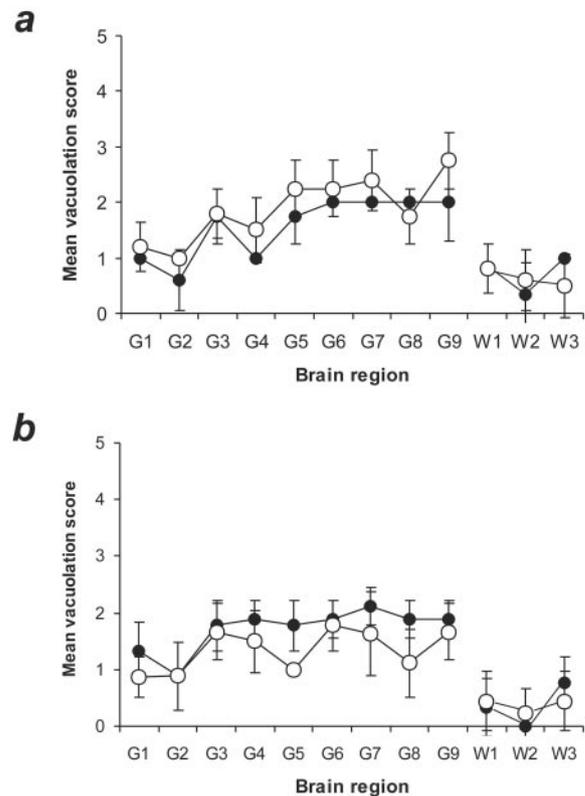

FIG. 3. Similar pathological targeting in the brains of terminally scrapie-affected CD40L$^{-/-}$ mice and C57BL/6 wild-type mice. Mice were inoculated with the ME7 scrapie strain by i.c. injection (a) or via skin scarification (b). Vacuolation in the brain was scored on a scale of 0 to 5 in the following gray-matter (G1 to G9) and white-matter (W1 to W3) areas: G1, dorsal medulla; G2, cerebellar cortex; G3, superior colliculus; G4, hypothalamus; G5, thalamus; G6, hippocampus; G7, septum; G8, retrosplenial and adjacent motor cortex; G9, cingulate and adjacent motor cortex; W1, inferior and middle cerebellar peduncles; W2, decussation of superior cerebellar peduncles; W3, cerebral peduncles. Each point represents the mean vacuolation score ± the standard deviation for groups of five to nine mice. Symbols: ●, C57BL/6 wild-type mice; ○, CD40L$^{-/-}$ mice.

coverslips were also exposed to scrapie-infected brain tissue and treated as described above. No PrP^{Sc} was detected on scrapie-exposed cell-free coverslips (data not shown), confirming that the PrP^{Sc} accumulations detected in Fig. 5a were cell associated. Antigens acquired by DCs usually quickly enter the lysosomal compartment, where they are broken down into peptides for presentation to lymphocytes in association with major histocompatibility complex class II (2). After extended cultivation of XS106 LC-like cells with scrapie (up to 96 h), the level of PrP^{Sc} detected in association with these cells appeared to decline (Fig. 5a). No significant effect on cell viability or metabolic activity was observed after exposure of the cells to scrapie-brain homogenate compared to those exposed to normal brain homogenate or medium alone as controls (data not shown). Thus, the reduction in the PrP^{Sc} associated with the XS106 LC-like cells was unlikely to be due to reduced cell viability.

In contrast to XS106 cells, XS52 cells are extremely "immature" in terms of their phenotype and function and have a poor
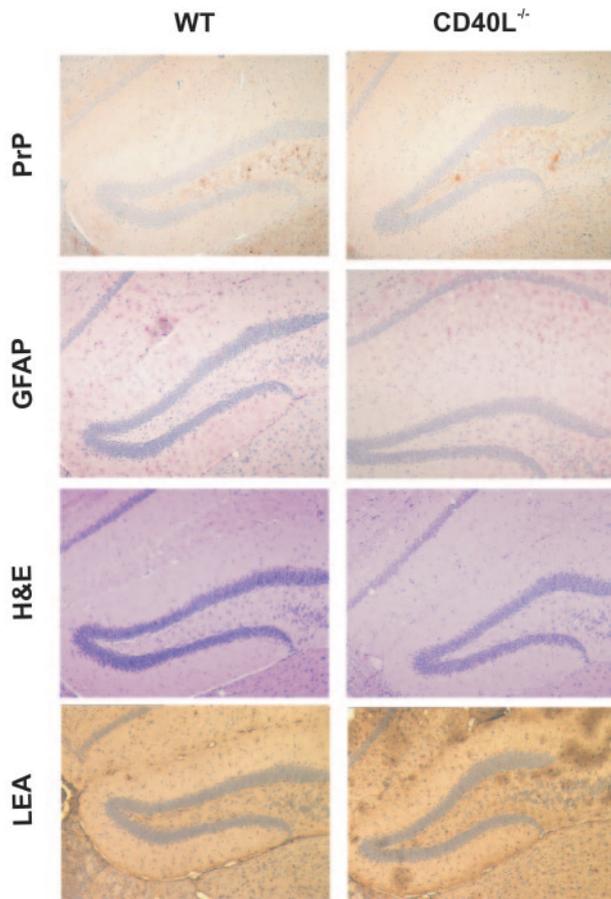
FIG. 4. Histological analysis of brain tissue from terminally scrapie-infected C57BL/6 wild-type (WT; left panels) and CD40L$^{-/-}$ mice (right panels) inoculated with scrapie by skin scarification. Large PrP accumulations (upper row; brown), reactive astrocytes expressing high levels of GFAP (second row; red), and spongiform pathology (hematoxylin and eosin; third row) were detected in the hippocampi of all mice that developed clinical signs of scrapie. Analysis of LEA-binding microglia (bottom row; brown) suggested that their activation was more pronounced in brains of CD40L$^{-/-}$ mice compared to wild-type mice. All sections were counterstained with hematoxylin (blue). Magnification, ×100.
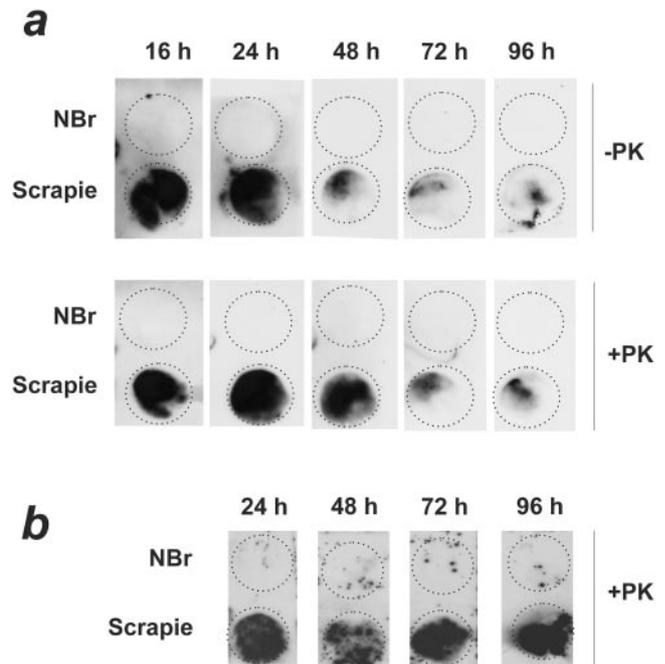

FIG. 5. Skin-derived LC-like cells degrade PrP^{Sc} in vitro. Monolayers of XS106 LC-like cells (a) or the highly immature cell line XS52 (b) were exposed to 10 μl of 10% scrapie-infected brain homogenate (scrapie) for 16 h. Duplicate sets of cultures were exposed to 10 μl of 10% uninfected normal brain homogenate (NBr) as a control. Monolayers were then washed to remove residual homogenate and incubated for the times indicated at 37°C in a 5% CO_2–air atmosphere. Levels of PrP^{Sc} associated with the cells were determined by cell blotting (5). Treatment of membranes in the presence (+) or absence (−) of proteinase K (PK) prior to immunostaining is indicated.

capacity to initiate antigen-specific immune responses in living animals (54, 59). In order to confirm that the ability of XS106 LC-like cells to degrade PrP^{Sc} was a property of cells with a phenotype typical of LCs and not a property of all in vitro-cultivated cell lines, parallel experiments were performed with the highly immature LC-like cell line XS52 as a negative control. Although these additional experiments demonstrated that, 24 h after inoculation with scrapie, XS52 LC-like cells had acquired high levels of PrP^{Sc} (Fig. 5b), after 96 h cultivation the level of PrP^{Sc} detected in association with these cells appeared to be similar to that observed at 24 h (Fig. 5b). Thus, taken together, these data suggest that "mature" XS106 LC-like cells, in contrast to highly "immature" XS52 cells, have the potential to acquire and degrade PrP^{Sc}.

DISCUSSION

In order to investigate the potential role of LCs in scrapie transportation from the skin to the draining lymph node, we utilized mouse models in which the migration of LCs from the skin was blocked (1, 40). We show that pharmacological blockade of LC migration (1) by treatment with an irreversible inhibitor of caspase-1 prior to inoculation with scrapie through the skin did not impair the early accumulation of infectivity in draining lymphoid tissue or delay subsequent neuroinvasion. The migration of LCs from the skin is also blocked in CD40L$^{-/-}$ mice (40). The early accumulation of infectivity in draining lymphoid tissues of these mice was likewise not impaired in the absence of LC migration from the skin. Together, these data suggest that LCs are not involved in TSE transport from the skin to lymphoid tissue. When wild-type mice and CD40L$^{-/-}$ mice were challenged with scrapie directly into the CNS, both strains of mice developed clinical signs of scrapie with similar incubation periods and exhibited similar CNS pathology. In contrast, after inoculation via skin scarification the disease incubation period was shorter in CD40L$^{-/-}$ mice than in wild-type mice. The shortened disease incubation period in CD40L$^{-/-}$ mice was unexpected and demonstrates that a CD40L-dependent process involved in impeding scrapie neuroinvasion was disrupted due to CD40L deficiency. Since DCs can process and degrade PrP^{Sc} in vitro (30), these data suggested to us that LCs might degrade scrapie in the skin. To address this, we exposed an epidermis-derived LC-like cell line (59) to scrapie in vitro. Our data suggest that in vitro-cultivated LCs are likewise able to acquire and degrade PrP^{Sc}. Taken

together, our studies suggest that LCs are not involved in scrapie transport to draining lymphoid tissue. However, these cells might have the potential to acquire and degrade scrapie in the skin.

TSE transport mechanisms from the site of exposure to the germinal centers in which they replicate are not known. We considered transport in association with migratory bone marrow-derived DCs a credible candidate mechanism since these cells sample antigens in the periphery and transport them to lymphoid tissues (2). DCs can also retain some protein antigens in native, nondegraded form (57). Recent research has demonstrated that bone marrow-derived DCs can acquire PrP^{Sc} in vitro (23, 30) and that a subpopulation of migratory DCs has the potential to transport intestinally injected PrP^{Sc} to mesenteric lymph nodes via the lymph (23). Others have shown that the prion protein fragment PrP$_{106-126}$ is a chemoattractant for monocyte-derived DCs (24). Despite these observations, direct demonstration of the involvement of DCs in the initial delivery of TSE agents to lymphoid tissues is lacking. Studies by Oldstone et al. (41) have suggested CD11c$^+$ DCs are not involved in peripheral TSE pathogenesis. However, in that study mice were inoculated with high doses of scrapie, which have been shown consistently to bypass the need for replication in lymphoid tissues in the same RML scrapie model (43) and our own ME7 scrapie model (16). Here we investigated the potential role of LCs in scrapie pathogenesis after inoculation via the skin with doses of ME7 scrapie equivalent to (10^4 ID$_{50}$ units) and much lower (10^3 ID$_{50}$ units) than those we have previously shown to require amplification in lymphoid tissues prior to neuroinvasion (31, 32, 51).

The cytokines interleukin-1β (IL-1β) and tumor necrosis factor alpha (TNF-α) play key roles in regulating the migration of LCs from the epidermis to the draining lymph node (12, 49). LC migration from the epidermis is blocked following specific inhibition of either of these cytokines (12). IL-1β is synthesized as an inactive 31-kDa precursor that is cleaved to release the active 17-kDa IL-1β molecule by the cysteine protease caspase-1 (52). In mice deficient in caspase-1 LC migration from the skin is impaired (1). Furthermore, treatment of skin with Ac-YVAD-cmk, an irreversible inhibitor of caspase-1 (19, 53), potently blocks both spontaneous and induced LC migration from the skin (1). Our data show that blockade of LC migration from the epidermis through treatment with Ac-YVAD-cmk prior to inoculation with scrapie did not affect the early accumulation of infectivity in draining ILNs since equally high levels were detected in tissues from both control and treated mice.

Treatment of mice with Ac-YVAD-cmk blocks induced LC migration from the skin by ca. 67% (1). Thus, the possibility that the magnitude of the Ac-YVAD-cmk-mediated inhibition of LC migration was insufficient to observe a measurable effect on pathogenesis deserves consideration. However, this hypothesis relies on the assumption that the 67% reduction in LC migration correlates directly to a 67% reduction in scrapie delivery. Our studies suggest that only a small subpopulation of intestinal DCs (0.5 to 5%) acquire and transport detectable levels of PrP^{Sc} from the gut lumen (23). Thus, it is possible that the majority of LC subpopulations, if involved in scrapie transportation, may be retained within the 67% that cannot migrate from the epidermis after Ac-YVAD-cmk treatment. After pe-

ripheral inoculation, it is likely that a portion of the inoculum is destroyed by the actions of phagocytic cells before it has the opportunity to begin replication in association with FDCs. The effects of this on pathogenesis are likely to be dose dependent, with small doses being more easily destroyed than higher doses, in which a greater portion would be retained. If a 67% reduction in LC migration did correlate directly to a 67% reduction in the initial scrapie delivery, it is possible that a further fraction may be degraded once it reached the draining lymph node, further reducing the inoculum titer.

With the above points in mind we are confident that the effects of Ac-YVAD-cmk-treatment on LC migration would be sufficient to cause a measurable effect on scrapie pathogenesis if these cells were involved. However, to further address this important issue, a mouse model was used in which LC migration from the skin is permanently blocked. In CD40L$^{-/-}$ mice, the number and morphology of LCs in the epidermis was normal but they did not migrate from the skin after stimulation (40). The defect in LC migration in CD40L$^{-/-}$ mice was associated with defective TNF-α production in the skin (40). When animals were inoculated with scrapie via the skin, high levels of infectivity were also detected within the ILNs of wild-type and CD40L$^{-/-}$ mice 49 days postinoculation. Thus, the early accumulation of scrapie in the draining lymphoid tissue was not impaired in mice whose LCs cannot migrate out of the epidermis. Therefore, these two approaches together suggest that the initial transportation of scrapie from the skin to draining lymphoid tissue occurs through an LC-independent mechanism.

The time point at which the tissues were assayed for infectivity accumulation is critical. If scrapie titers were to peak much sooner than the time they are analyzed it may not be possible to demonstrate a reduced early accumulation in mice with blocked LC migration since sufficient time may have been provided for a reduced scrapie dose to reach peak levels before analysis. Our unpublished observations suggest that after inoculation with scrapie by skin scarification the infectivity levels in the draining ILN begin to peak around 49 days postinoculation and subsequently plateau. If the delivery of scrapie infectivity to the draining lymph node was reduced in the absence of migratory LCs, these data suggest that it would have been possible to demonstrate a reduced accumulation of infectivity in draining ILNs 49 days after inoculation since infectivity levels in tissues from control mice would only just have started to approach peak levels.

Every effort was taken at the time of scarification to avoid causing damage to the dermis or drawing blood to prevent the leakage of infectivity into the bloodstream during inoculation. If scrapie infectivity had leached into the bloodstream, a need for LCs in transportation to lymphoid tissues would obviously have been bypassed. Analysis of spleen tissue 49 days postinoculation failed to detect infectivity in tissues collected from the same wild-type and CD40L$^{-/-}$ mice. These data therefore suggest that the initial transmission of scrapie from the skin to lymphoid tissues does not occur via the bloodstream, which would have resulted in a widespread dissemination of infectivity throughout the lymphoid system. Spleen tissue collected for immunoblot analysis from terminally affected wild-type and CD40L$^{-/-}$ mice detected large accumulations of PrP^{Sc}. Therefore, following inoculation via the skin, infectivity is first prop-

agated to the draining lymph node via the lymphatics in an LC-independent manner and subsequently distributed to the spleen, probably via the bloodstream.

Mice deficient in CD40L are incapable of mounting T-lymphocyte-dependent humoral immune responses (58). Although mature FDC networks surrounded by B cells were detected in the spleens of CD40L$^{-/-}$ mice, germinal centers containing PNA-binding B lymphocytes were absent. After inoculation by skin scarification CD40L$^{-/-}$ mice accumulated levels of PrP^{Sc} and infectivity in their lymphoid tissues comparable to wild-type mice, despite an absence of germinal centers. Thus, the absence of PNA-positive germinal centers in CD40L$^{-/-}$ mice does not affect the ability of their lymphoid tissues to accumulate PrP^{Sc} and infectivity after exposure to the ME7 scrapie strain. These data are consistent with previous studies utilizing IL-6$^{-/-}$ mice that also have diminished germinal centers but mature FDC networks in the spleen (29). After peripheral inoculation with ME7 scrapie, spleens of IL-6$^{-/-}$ mice accumulated levels of PrP^{Sc} and scrapie infectivity comparable to those in the spleens of wild-type mice and maintained these levels for the duration of the disease (33). Since deficiencies in T lymphocytes (26, 27) or circulating immunoglobulins (28) do not affect scrapie pathogenesis, it is likewise unlikely that the impaired T-lymphocyte-dependent humoral immune responses in CD40L$^{-/-}$ mice (58) affect pathogenesis.

Congruent with the observation that the early accumulation of scrapie infectivity in lymphoid tissues was not impaired in the absence of LC migration, further studies demonstrated that scrapie susceptibility was not reduced in mice with blocked LC migration. When challenged with scrapie by skin scarification, CD40L$^{-/-}$ mice succumbed to clinical disease with a significantly shorter incubation period than wild-type mice (Table 2). The shortened incubation period in CD40L$^{-/-}$ mice was unexpected since a similar affect on scrapie pathogenesis was not observed after inhibition of LC migration by topical treatment with a caspase-1 inhibitor (Table 1). CD40 signaling on neurons has been shown to play a physiological role in promoting neuronal maintenance and survival (50). Thus, the shortened scrapie incubation period observed in peripherally inoculated CD40L$^{-/-}$ mice might have been due to an increased susceptibility of CD40L-deficient neurons to TSE-induced neurodegeneration. After inoculation of wild-type and CD40L$^{-/-}$ mice with scrapie directly into the CNS (i.c. injection), all mice developed clinical disease with similar incubation periods. Furthermore, the pathological targeting of the TSE-induced vacuolation (Fig. 3), PrP^{Sc} accumulation, or gliosis within the brain was not significantly different between mouse strains, although microglia activation appeared to be more pronounced in CD40L$^{-/-}$ mice. Despite this apparent increase in microglia activation, the magnitude and distribution of the disease-specific vacuolation in 12 different brain regions were similar between CD40L$^{-/-}$ and wild-type mice. These data therefore demonstrate that the CD40-CD40L signaling pathway does not play a critical role in the cerebral pathogenesis of ME7 scrapie. Therefore, the shortened incubation period observed in peripherally inoculated CD40L$^{-/-}$ mice was most likely due to the absence of a CD40L-dependent mechanism in the periphery, which may be involved in impeding scrapie pathogenesis. It may also be possible that

CD40L deficiency affects the permeability of peripheral neurons to TSEs influencing uptake and neuroinvasion.

In contrast to data described in the present study, a recent report suggests the CD40-CD40L signaling pathway is involved in the development and progression of CNS disease after inoculation with the 139A scrapie strain (8). In that study, CD40L$^{-/-}$ mice inoculated with 139A scrapie directly into the CNS (i.c. injection) succumbed to disease 40 days earlier than did wild-type control mice. Congruent with the findings in our study, no significant differences in the extent of disease-specific PrP-deposition or GFAP-expressing astrocytes were detected in the brains of CD40L$^{-/-}$ and wild-type mice, although microglia activation appeared to be more pronounced in CD40L$^{-/-}$ mice. However, the magnitude of the disease-associated vacuolation detected in the brains of CD40L$^{-/-}$ mice was also more pronounced than in wild-type mice (8). This is in contrast to data from our studies in which the magnitude and distribution of the pathological targeting of the vacuolation in CD40L$^{-/-}$ mice were remarkably similar to the findings in wild-type mice after inoculation either directly into the CNS (i.c.) or via the skin (Fig. 3). In wild-type mice the distribution and magnitude of the pathological targeting of the vacuolation within the brain differs significantly between the 139A and ME7 scrapie strains: for example, the 139A scrapie strain induces stronger vacuolation in white matter. Therefore, these two studies, considered together, suggest that it is possible that the effects of CD40L on scrapie pathogenesis within the brain are strain dependent.

CD40-CD40L interactions have a diverse range of activities within the immune system, and further studies are necessary to determine the precise effect of the blockade of this signaling pathway on peripheral pathogenesis of ME7 scrapie. Apart from a lack of PNA-binding germinal centers (58), there was little evidence of disrupted lymphoid architecture in the lymphoid tissues of CD40L$^{-/-}$ mice. Thus, the reduced incubation period was unlikely to be due to effects on lymphoid architecture, such as the repositioning of splenic FDCs in close association with peripheral nerves as recently shown in mice deficient in the CXCR5 chemokine receptor (42). CD40-CD40L interactions provide important signals for optimal macrophage activation, and CD40L deficiency increases susceptibility to certain intracellular pathogens (9, 36, 48). For example, macrophages from *Leishmania amazonensis*-infected CD40L$^{-/-}$ mice contain high parasite burdens and are unable to effectively control the parasitemia (48). Since previous studies suggest that macrophages may sequester and destroy scrapie infectivity (4, 10, 11), it is reasonable to speculate that in the absence of CD40-CD40L signaling in CD40L$^{-/-}$ mice the clearance of scrapie infectivity by cells such as macrophages is likewise inhibited. For example, studies from Prinz et al. (43) demonstrate that, in the absence of TNF receptor 1 signaling, scrapie replication can occur in macrophages. Following uptake by DCs, antigens rapidly enter the lysosomal compartment, where they are broken down into peptides for presentation to lymphocytes in association with major histocompatibility complex class II (2). A recent study suggests that DCs may handle TSE agents in a similar manner, since bone marrow-derived DCs are able to process and degrade PrP^{Sc} after in vitro exposure (30). Our studies also show that in vitro-cultivated XS106 LC-like cells have the potential to acquire and degrade

MOHAN ET AL.J. VIROL.

PrP^{Sc}. Another interpretation of these observations may be that, after the uptake of PrP^{Sc} by XS106 LC-like cells, subsequent processing and/or catabolism of PrP^{Sc} masks the 8H4 epitope. However, whatever the effects of XS106 cells on PrP^{Sc} were, further experiments confirmed that this was not a property of all in vitro-cultivated cell lines since the highly immature cell line XS52 was unable to degrade PrP^{Sc}. Thus, these data suggest that highly efficient antigen-processing LCs might be impeded in processing scrapie in CD40L-deficient mice. Inhibition of CD40L-dependent clearance mechanisms might allow infectivity to accumulate earlier in draining lymphoid tissue, shortening the disease incubation period. Treatments that modulate this CD40L-dependent protective mechanism might provide an effective therapeutic strategy for early intervention in TSE pathogenesis.

The data presented here suggest that LCs are not involved in the transportation of scrapie from the skin to lymphoid tissues. However, these data do suggest that a CD40-CD40L-dependent mechanism is involved in impeding scrapie neuroinvasion. The precise mechanism by which scrapie infectivity is transported from the skin to lymphoid tissues remains to be identified. Since macrophages are most likely involved in the degradation of infectivity (4, 10, 11), it is possible that scrapie infectivity is transported in a cell-free manner. Soon after entering the host antigens are rapidly opsonized by complement components. Recent research has shown that complement components play an important role in the localization of scrapie to lymphoid tissues (28, 31), suggesting TSE agents might be delivered to lymphoid tissues as cell-free complement-bound complexes. Understanding the earliest peripheral mechanisms involved in the transportation or degradation of scrapie will be important in the development of therapeutic strategies to combat these fatal neurodegenerative diseases.

ACKNOWLEDGMENTS

We thank Richard Groves (Department of Dermatology, Chelsea, and Westminster Hospital, London, United Kingdom) for helpful discussions and guidance concerning the caspase inhibitor treatments; Irene McConnell, Mary Brady, Lorraine Gray, and Susan Denham (Neuropathogenesis Unit, Institute for Animal Health, Edinburgh, United Kingdom) for excellent technical support; David Gray (University of Edinburgh, Edinburgh, United Kingdom) for provision of the CD40L$^{-/-}$ mice; Man-Sun Sy (Case Western Reserve University School of Medicine, Cleveland, Ohio) for provision of 8H4 monoclonal antiserum; and Akira Takashima (University of Texas Southwestern Medical Centre, Dallas, Tex.) for provision of the XS106, XS52, and NS47 cell lines.

This study was supported by funding from the Medical Research Council and the Biotechnology and Biological Sciences Research Council.

REFERENCES

1. **Antonopoulos, C., M. Cumberbatch, R. J. Dearman, R. J. Daniel, I. Kimber, and R. W. Groves.** 2001. Functional caspase-1 is required for Langerhans cell migration and optimal contact sensitization in mice. J. Immunol. **166:**3672–3677.
2. **Banchereau, J., F. Briere, C. Caux, J. Davoust, S. Lebecque, Y. J. Liu, B. Pulendran, and K. Palucka.** 2000. Immunobiology of dendritic cells. Annu. Rev. Immunol. **18:**767–811.
3. **Bartz, J. C., A. E. Kincaid, and R. A. Bessen.** 2003. Rapid prion neuroinvasion following tongue infection. J. Virol. **77:**583–591.
4. **Beringue, V., M. Demoy, C. I. Lasmezas, B. Gouritin, C. Weingarten, J.-P. Deslys, J.-P. Adreux, P. Couvreur, and D. Dormont.** 2000. Role of spleen macrophages in the clearance of scrapie agent early in pathogenesis. J. Pathol. **190:**495–502.
5. **Bosque, P. J., and S. B. Prusiner.** 2000. Cultured cell sublines highly susceptible to prion infection. J. Virol. **74:**4377–4386.
6. **Brown, K. L., K. Stewart, D. Ritchie, N. A. Mabbott, A. Williams, H. Fraser, W. I. Morrison, and M. E. Bruce.** 1999. Scrapie replication in lymphoid tissues depends on PrP-expressing follicular dendritic cells. Nat. Med. **5:**1308–1312.
7. **Bruce, M. E., R. G. Will, J. W. Ironside, I. McConnell, D. Drummond, A. Suttie, L. McCardle, A. Chree, J. Hope, C. Birkett, S. Cousens, H. Fraser, and C. J. Bostock.** 1997. Transmissions to mice indicate that "new variant" CJD is caused by the BSE agent. Nature **389:**498–501.
8. **Burwinkel, M., A. Schwarz, C. Riemer, J. Schultz, F. van Landeghem, and M. Baier.** 2004. Rapid disease development in scrapie-infected mice deficient for CD40 ligand. EMBO Rep. **5:**527–531.
9. **Campbell, K. A., P. J. Ovendale, M. K. Kennedy, W. C. Fanslow, S. G. Reed, and C. R. Maliszewski.** 1996. CD40 ligand is required for protective cell-mediated immunity to *Leishmania major*. Immunity **4:**283–289.
10. **Carp, R. I., and S. M. Callahan.** 1982. Effect of mouse peritoneal macrophages on scrapie infectivity during extended in vitro incubation. Intervirology **17:**201–207.
11. **Carp, R. I., and S. M. Callahan.** 1981. In vitro interaction of scrapie agent and mouse peritoneal macrophages. Intervirology **16:**8–13.
12. **Cumberbatch, M., R. J. Dearman, and I. Kimber.** 1997. Langerhans cells require signals from both tumour necrosis factor-α and interleukin-1β for migration. Immunology **92:**388–396.
13. **Enari, M., E. Flechsig, and C. Weissmann.** 2001. Scrapie prion protein accumulation by scrapie-infected neuroblastoma cells abrogated by exposure to a prion protein antibody. Proc. Natl. Acad. Sci. USA **98:**9295–9299.
14. **Endres, R., M. B. Alimzhanov, T. Plitz, A. Futterer, M. H. Kosco-Vilbois, S. A. Nedospasov, K. Rajewsky, and K. Pfeffer.** 1999. Mature follicular dendritic cell networks depend on expression of lymphotoxin β receptor by radioresistant stromal cells and of lymphotoxin β and tumour necrosis factor by B cells. J. Exp. Med. **189:**159–168.
15. **Farquhar, C. F., J. Dornan, R. A. Somerville, A. M. Tunstall, and J. Hope.** 1994. Effect of *Sinc* genotype, agent isolate and route of infection on the accumulation of protease-resistant PrP in non-central nervous system tissues during the development of murine scrapie. J. Gen. Virol. **75:**495–504.
16. **Fraser, H., K. L. Brown, K. Stewart, I. McConnell, P. McBride, and A. Williams.** 1996. Replication of scrapie in spleens of SCID mice follows reconstitution with wild-type mouse bone marrow. J. Gen. Virol. **77:**1935–1940.
17. **Fraser, H., and A. G. Dickinson.** 1973. Agent-strain differences in the distribution and intensity of gray matter vacuolation. J. Comp. Pathol. **83:**29–40.
18. **Fraser, H., and A. G. Dickinson.** 1968. The sequential development of the brain lesions of scrapie in three strains of mice. J. Comp. Pathol. **78:**301–311.
19. **Garcia Calvo, M., E. P. Peterson, B. Leiting, R. Ruel, D. W. Nicholson, and N. A. Thornberry.** 1998. Inhibition of human caspases by peptide-based and macromolecular inhibitors. J. Biol. Chem. **273:**32608–32613.
20. **Glatzel, M., F. L. Heppner, K. M. Albers, and A. Aguzzi.** 2001. Sympathetic innervation of lymphoreticular organs is rate limiting for prion neuroinvasion. Neuron **31:**25–34.
21. **Hill, A. F., R. J. Butterworth, S. Joiner, G. Jackson, M. N. Rossor, D. J. Thomas, A. Frosh, N. Tolley, J. E. Bell, M. Spencer, A. King, S. Al-Sarraj, J. W. Ironside, P. L. Lantos, and J. Collinge.** 1999. Investigation of variant Creutzfeldt-Jakob disease and other prion diseases with tonsil biopsy samples. Lancet **353:**183–189.
22. **Hill, A. F., M. Desbruslais, S. Joiner, K. C. L. Sidle, I. Gowland, and J. Collinge.** 1997. The same prion strain causes vCJD and BSE. Nature **389:**448–450.
23. **Huang, F.-P., C. F. Farquhar, N. A. Mabbott, M. E. Bruce, and G. G. MacPherson.** 2002. Migrating intestinal dendritic cells transport PrP^{Sc} from the gut. J. Gen. Virol. **83:**267–271.
24. **Kaneider, N. C., A. Kaser, S. Dunzendorfer, H. Tilg, and C. J. Wiedermann.** 2003. Sphingosine kinase-dependent migration of immature dendritic cells in response to neurotoxic prion protein fragment. J. Virol. **77:**5535–5539.
25. **Kapasi, Z. F., C. F. Burton, L. D. Schultz, J. G. Tew, and A. K. Szakal.** 1993. Induction of functional follicular dendritic cell development in severe combined immunodeficiency mice. J. Immunol. **150:**2648–2658.
26. **Klein, M. A., R. Frigg, E. Flechsig, A. J. Raeber, U. Kalinke, H. Bluethman, F. Bootz, M. Suter, R. M. Zinkernagel, and A. Aguzzi.** 1997. A crucial role for B cells in neuroinvasive scrapie. Nature **390:**687–691.
27. **Klein, M. A., R. Frigg, A. J. Raeber, E. Flechsig, I. Hegyi, R. M. Zinkernagel, C. Weissmann, and A. Aguzzi.** 1998. PrP expression in B lymphocytes is not required for prion neuroinvasion. Nat. Med. **4:**1429–1433.
28. **Klein, M. A., P. S. Kaeser, P. Schwarz, H. Weyd, I. Xenarios, R. M. Zinkernagel, M. C. Carroll, J. S. Verbeek, M. Botto, M. J. Walport, H. Molina, U. Kalinke, H. Acha-Orbea, and A. Aguzzi.** 2001. Complement facilitates early prion pathogenesis. Nat. Med. **7:**488–492.
29. **Kopf, M., S. Herren, M. V. Wiles, M. B. Pepys, and M. H. Kosco-Vilbois.** 1998. Interleukin 6 influences germinal center development and antibody production via a contribution of C3 complement component. J. Exp. Med. **188:**1895–1906.
30. **Luhr, K. M., R. P. A. Wallin, H.-G. Ljunggren, P. Löw, A. Tarabulos, and K. Kristensson.** 2002. Processing and degradation of exogenous prion protein by CD11c^{+} myeloid dendritic cells in vitro. J. Virol. **76:**12259–12264.

31. **Mabbott, N. A., M. E. Bruce, M. Botto, M. J. Walport, and M. B. Pepys.** 2001. Temporary depletion of complement component C3 or genetic deficiency of C1q significantly delays onset of scrapie. Nat. Med. **7:**485–487.

32. **Mabbott, N. A., F. Mackay, F. Minns, and M. E. Bruce.** 2000. Temporary inactivation of follicular dendritic cells delays neuroinvasion of scrapie. Nat. Med. **6:**719–720.

33. **Mabbott, N. A., A. Williams, C. F. Farquhar, M. Pasparakis, G. Kollias, and M. E. Bruce.** 2000. Tumor necrosis factor-alpha-deficient, but not interleukin-6-deficient, mice resist peripheral infection with scrapie. J. Virol. **74:**3338–3344.

34. **Mabbott, N. A., J. Young, I. McConnell, and M. E. Bruce.** 2003. Follicular dendritic cell dedifferentiation by treatment with an inhibitor of the lymphotoxin pathway dramatically reduces scrapie susceptibility. J. Virol. **77:**6845–6854.

35. **MacDonald, G. H., and R. E. Johnston.** 2000. Role of dendritic cell targeting in Venezuelan equine encephalitis virus pathogenesis. J. Virol. **62:**914–922.

36. **Marriott, I., E. K. Thomas, and K. L. Bost.** 1999. CD40-CD40 ligand interactions augment survival of normal mice, but not CD40 ligand knockout mice, challenged orally with *Salmonella dublin*. Infect. Immun. **67:**5253–5257.

37. **McBride, P., P. Eikelenboom, G. Kraal, H. Fraser, and M. E. Bruce.** 1992. PrP protein is associated with follicular dendritic cells of spleens and lymph nodes in uninfected and scrapie-infected mice. J. Pathol. **168:**413–418.

38. **Meyer, R. K., M. P. McKinley, K. A. Bowman, M. B. Braunfeld, R. A. Barry, and S. B. Prusiner.** 1986. Separation and properties of cellular and scrapie prion proteins. Proc. Natl. Acad. Sci. USA **83:**2310–2314.

39. **Montrasio, F., R. Frigg, M. Glatzel, M. A. Klein, F. Mackay, A. Aguzzi, and C. Weissmann.** 2000. Impaired prion replication in spleens of mice lacking functional follicular dendritic cells. Science **288:**1257–1259.

40. **Moodycliffe, A. M., V. Shreedhar, S. E. Ullrich, J. Walterscheid, C. Bucana, M. L. Kripke, and L. Flores-Romo.** 2000. CD40-CD40 ligand interactions in vivo regulate migration of antigen-bearing dendritic cells from the skin to draining lymph nodes. J. Exp. Med. **191:**2011–2020.

41. **Oldstone, M. B. A., R. Race, D. Thomas, H. Lewicki, D. Homman, S. Smelt, A. Holz, P. Koni, D. Lo, B. Chesebro, and R. Flavell.** 2002. Lymphotoxin-α- and lymphotoxin-β-deficient mice differ in susceptibility to scrapie: evidence against dendritic cell involvement. J. Virol. **76:**4357–4363.

42. **Prinz, M., M. Heikenwalder, T. Junt, P. Schwarz, M. Glatzel, F. L. Heppner, Y.-X. Fu, M. Lipp, and A. Aguzzi.** 2003. Positioning of follicular dendritic cells within the spleen controls prion neuroinvasion. Nature **425:**957–962.

43. **Prinz, M., F. Montrasio, M. A. Klein, P. Schwarz, J. Priller, B. Odermatt, K. Pfeffer, and A. Aguzzi.** 2002. Lymph nodal prion replication and neuroinvasion in mice devoid of follicular dendritic cells. Proc. Natl. Acad. Sci. USA **99:**919–924.

44. **Prusiner, S. B., D. C. Bolton, D. F. Groth, K. A. Bowman, S. P. Cochran, and M. P. McKinley.** 1982. Further purification and characterisation of scrapie prions. Biochemistry **21:**6942–6950.

45. **Reece, J. C., A. J. Handley, E. J. Anstee, W. A. Morrison, S. M. Crowe, and P. U. Cameron.** 1998. HIV-1 selection by epidermal dendritic cells during transmission across human skin. J. Exp. Med. **187:**1623–1631.

46. **Ryan, S., L. Tiley, I. McConnell, and B. Blacklaws.** 2000. Infection of dendritic cells by the maedi-visna lentivirus. J. Virol. **74:**10096–10103.

47. **Sigurdson, C. J., E. S. Williams, M. W. Miller, T. R. Spraker, K. I. O'Rourke, and E. A. Hoover.** 1999. Oral transmission and early lymphoid tropism of chronic wasting disease PrP^{res} in mule deer fawns (*Odocoileus hemionus*). J. Gen. Virol. **80:**2757–2764.

48. **Soong, L., J. C. Xu, I. S. Grewal, P. Kima, J. Sun, B. J. Longley, Jr., N. H. Ruddle, D. McMahon-Pratt, and R. A. Flavell.** 1996. Disruption of CD40-CD40 ligand interactions results in an enhanced susceptibility to *Leishmania amazonensis* infection. Immunity **4:**263–273.

49. **Stoitzner, P., M. Zanella, U. Ortner, M. Lukas, A. Tagwerker, K. Janke, M. B. Lutz, G. Schuler, B. Echtenacher, B. Ryffel, F. Koch, and N. Romani.** 1999. Migration of Langerhans cells and dermal dendritic cells in skin organ cultures: augmentation by TNF-α and IL-1β. J. Leukoc. Biol. **66:**462–470.

50. **Tan, J., T. Town, T. Mori, D. Obregon, Y. Wu, A. DelleDonne, A. Rojiani, F. Crawford, R. A. Flavell, and M. Mullan.** 2002. CD40 is expressed and functional on neuronal cells. EMBO J. **21:**643–652.

51. **Taylor, D. M., I. McConnell, and H. Fraser.** 1996. Scrapie infection can be established readily through skin scarification in immunocompetent but not immunodeficient mice. J. Gen. Virol. **77:**1595–1599.

52. **Thornberry, N. A., H. G. Bull, J. R. Calaycay, K. T. Chapman, A. D. Howard, M. J. Kostura, D. K. Miller, S. M. Molineaux, J. R. Weidner, J. Aunins, et al.** 1992. A novel heterodimeric cysteine protease is required for interleukin-1b processing in monocytes. Nature **356:**768–784.

53. **Thornberry, N. A., E. P. Peterson, J. J. Zhao, A. D. Howard, P. R. Griffin, and K. T. Chapman.** 1994. Inactivation of interleukin-1β converting enzyme by peptide (acyloxy)methyl ketones. Biochemistry **33:**3934–3940.

54. **Timares, L., A. Takashima, and S. A. Johnston.** 1998. Quantitative analysis of the immunopotency of genetically transfected dendritic cells. Proc. Natl. Acad. Sci. USA **95:**13147–13152.

55. **van Keulen, L. J. M., B. E. C. Schreuder, R. H. Meloen, G. Mooij-Harkes, M. E. W. Vromans, and J. P. M. Langeveld.** 1996. Immunohistological detection of prion protein in lymphoid tissues of sheep with natural scrapie. J. Clin. Microbiol. **34:**1228–1231.

56. **Wu, S.-J. L., G. Grouard-Vogel, W. Sun, J. R. Mascola, E. Brachtel, R. Putvatana, M. K. Louder, L. Filgueira, M. A. Marovich, H. K. Wong, A. Blauvelt, G. S. Murphy, M. L. Robb, B. L. Innes, D. L. Birx, C. G. Hayes, and S. Schlesinger Frankel.** 2000. Human skin Langerhans cells are targets of dengue virus infection. Nat. Med. **6:**816–820.

57. **Wykes, M., A. Pombo, C. Jenkins, and G. G. MacPherson.** 1998. Dendritic cells interact directly with Naive B lymphocytes to transfer antigen and initiate class switching in a primary T-dependent response. J. Immunol. **161:**1313–1319.

58. **Xu, J., T. M. Foy, J. D. Laman, E. A. Elliot, J. J. Dunn, T. J. Waldschmidt, R. Elsemore, R. J. Noelle, and R. A. Flavell.** 1994. Mice deficient for the CD40 ligand. Immunity **1:**423–431.

59. **Xu, S., K. Ariizumi, G. Caceres-Dittmar, D. Edelbaum, K. Hashimoto, P. R. Bergstresser, and A. Takashima.** 1995. Successive generation of antigen-presenting dendritic cell lines from murine epidermis. J. Immunol. **154:**2697–2705.

60. **Yamada, N., and S. I. Katz.** 1999. Generation of mature dendritic cells from CD14^{+} cell line (XS52) by IL-4, TNF-α, IL-1β, and agonistic anit-CD40 monoclonal antibody. J. Immunol. **163:**5331–5337.

61. **Zanusso, G., D. Liu, S. Ferrari, I. Hegyi, X. Yin, A. Aguzzi, S. Hornemann, S. Liemann, R. Glockshuber, J. C. Manson, P. Brown, R. B. Petersen, P. Gambetti, and M.-S. Sy.** 1998. Prion protein expression in different species: analysis with a panel of new mAbs. Proc. Natl. Acad. Sci. USA **95:**8812–8816.